THE JOURNAL OF PHYSICAL CHEMISTRY C

Article

pubs.acs.org/JPCC

Intramolecular Cooperative Effects in Multichromophoric Cavitands Exhibiting Nonlinear Optical Properties

Zsolt Csók,*[,†] Péter Szuroczki,[‡] László Kollár,[‡,§] Hoang Minh Ngo,[∥] Isabelle Ledoux-Rak,[∥,¶] Naidel A. M. S. Caturello,[†] and Rodrigo Q. Albuquerque[†]

[†]São Carlos Institute of Chemistry, University of São Paulo, Avenida Trab. São-carlense 400, 13560-970 São Carlos (SP), Brazil

[‡]Department of Inorganic Chemistry and MTA-PTE Research Group for Selective Chemical Syntheses, University of Pécs, Ifjúság 6, H-7624 Pécs, Hungary

[§]János Szentágothai Research Center, Ifjúság 20, H-7624 Pécs, Hungary

[∥]Quantum and Molecular Photonics Laboratory (LPQM-ENS), École Normale Supérieure de Cachan, 61 Avenue du Président Wilson, F-94230 Cachan, France

Supporting Information

ABSTRACT: We report on the design, synthesis, and characterization of a new class of multichromophoric cavitands based on resorcin[4]arenes. The novel compounds have exhibited high values of second-order nonlinear optical (NLO) properties, as evidenced by electric-field-induced second harmonic generation (EFISHG) measurements. Theoretical calculations indicate the presence of edge-to-face T-shaped interactions between the aromatic building blocks within these multichromophoric systems, which is further supported by the detection of hypsochromic shifts in UV−vis and upfield aromatic chemical shifts in ^{1}H NMR. We proved for the first time that the gain in the quadratic hyperpolarizabilities of multichromophoric NLO macrocycles, originating from the near parallel orientations of the subchromophores, can be partially suppressed if the distance between the dipolar subunits falls into a specific range, where intramolecular cooperative and/or collective effects are operative. Our finding will contribute to the better understanding of the phenomenon of cooperativity in new molecular materials with promising NLO properties.

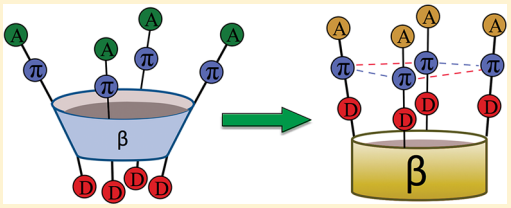

1. INTRODUCTION

Organic molecules exhibiting high second-order nonlinear optical (NLO) properties contain both electron-donating and electron-accepting groups connected via a conjugated π-system (D−π−A molecules).[1−6] These compounds are promising candidates for various NLO applications such as optical communication (signal processing, frequency generation), optical data storage, electronic and photonic devices, and quantum machines.[1−3] The key feature of second-order NLO-active molecules is a noncentrosymmetric, highly polarizable structure that is expressed as the second-order (quadratic) nonlinear polarizability or the first hyperpolarizability tensor (β). Since the quadratic hyperpolarizability increases almost linearly with the number of chromophores,[7] the preparation of multichromophoric systems favoring an intramolecular noncentrosymmetric order is an attractive way to attain remarkable NLO activities.

Donor−acceptor functionalized calix[4]arenes, pioneered by Reinhoudt et al.,[8−11] gave rise to multichromophoric materials with advanced NLO properties.[12,13] Some illustrative examples are depicted in Chart 1: tetra(nitro)calix[4]arene (**1**), tetrakis(nitrostilbene)calix[4]arene (**2**), tetrakis(phenylethynyl)calix[4]arene (**3a**), tetrakis(4-trifluoromethylphenylethynyl)calix[4]arene (**3b**), and tetrakis(4-nitrophenylethynyl)calix[4]arene (**3c**).

Calixarenes display a certain degree of conformational mobility in solution, even if a relatively stable cone conformation is adopted.[14,15] The rotation around the methylene bridges generates a "breathing" motion that leads to a dynamic equilibrium between the two possible terminal positions of the phenolic subunits. Although large hyperpolarizabilities are expected from the intramolecular order exhibited by these compounds, the conformational mobility in solution causes nonparallel orientations of the dipolar subunits. Hence, the increase of the cone opening angle may cancel, at least partially, the enhancement in the β value of the multichromophoric molecule along the dipolar axis. Similarly, the relative orientation of the single NLO-active subunits was found to be the key factor for controlling the second-order NLO properties of cyclotetrasiloxane macrocycles decorated with four push−pull organic polar tails.[5] Since these multichromophoric materials have been regarded as a collection of isolated subchromophores, their NLO behaviors were explained by the additive oriented-gas model, in which intramolecular interactions are fully neglected. In accordance with this approximation, the dipolar quadratic hyperpolarizability of a

Received: March 30, 2015
Revised: May 11, 2015
Published: May 14, 2015

DOI: 10.1021/acs.jpcc.5b03047
J. Phys. Chem. C 2015, 119, 12608−12615

Chart 1. Typical Examples of Conjugated Calix[4]arenes Displaying Enhanced NLO Activities

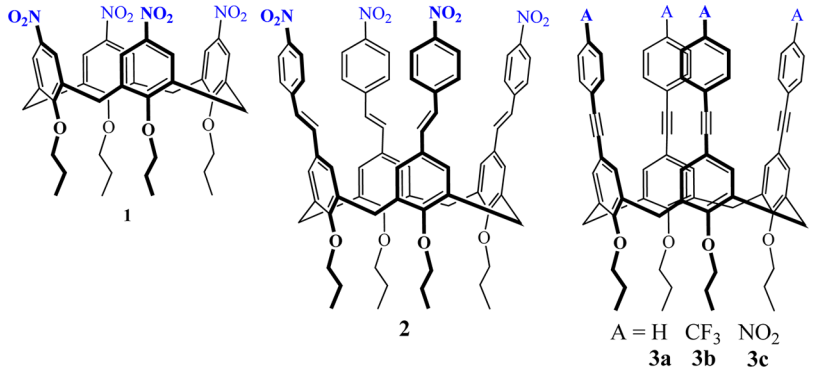

multichromophoric system (β_{multi}) in the direction of the dipole axis can be simply expressed as a tensorial summation of the individual contributions of all NLO activities of the non-interacting monochromophoric subunits (β_{mono}):

$$\beta_{multi} = N(\cos^3\theta)\beta_{mono} \quad (1)$$

where N is the number of the chromophoric subunits and θ is the opening angle, i.e., the angle between the individual monochromophoric subunits and the dipole axis of the multichromophoric molecule. The permanent dipole moment (μ_{multi}) along the molecular axis can be expressed as

$$\mu_{multi} = N(\cos\theta)\mu_{mono} \quad (2)$$

The relevant parameter for the evaluation of the NLO performance of a dipolar multichromophore is the scalar product of the permanent dipole moment (μ_{multi}) and the dipolar, vectorial part of the hyperpolarizability tensor (β_{multi}):[5,11]

$$\mu\beta_{multi} = N^2(\cos^4\theta)\mu\beta_{mono} \quad (3)$$

In a seminal theoretical work,[16] Datta et al. critically investigated the validity of the oriented-gas behavior of **3a–c** using an essential-state model developed for interacting polar–polarizable molecules of push–pull chromophores,[17−19] supported by density functional theory calculations. The NLO properties of these calixarenes were found to be far from additive: the hyperpolarizabilities were suppressed with respect to the prediction of the oriented-gas model. The maximum damping in β was observed for the conformer in which the orientations of the dipolar subunits are completely parallel ($\theta = 0°$). For this conformation, the model predicted a reduction of up to 30% from the oriented-gas model. This nonadditive NLO behavior was clearly explained by the effects of intramolecular electrostatic interactions between the dipolar subchromophores. Furthermore, previous theoretical investigations on each conformer of **1**[20] as well as on the supramolecular dimers of para-nitroanilines[21] have revealed that the hyperpolarizabilities decrease for distances in the "destructive" range of 3.5–9.0 Å due to face-to-face interactions between the aromatic π-systems.

Resorcin[4]arenes, representing another fascinating class of molecular hosts, are acid-catalyzed condensation products of resorcinol and aldehydes.[22,23] The enhanced rigidity of cavitands (**4**) based on resorcin[4]arenes originates from an additional intramolecular covalent bridging (n = 1, 2, 3) between the vicinal, phenolic OH groups (Chart 2).[24] The variation of the R_1 group at the lower rim ("feet") and R_2 at the upper rim of the cavitand enables one to access a wide range of interesting derivatives. It has been recently demonstrated that a tetraiodocavitand (**4**, n = 1, $R_1 = CH_3$, $R_2 = CH_2O$–4-I–C_6H_4) precursor has opened up new possibilities for the preparation of deep cavitands. For example, palladium-catalyzed cross-coupling and carbonylation reactions as well as copper-catalyzed azide–alkyne cycloadditions (CuAAC) were shown to be excellent synthetic tools for the molecular enlargement of the cavitand scaffold.[25−28]

Chart 2. General Molecular Structure of Cavitands Based on Resorcin[4]arenes, Where n = 1–3

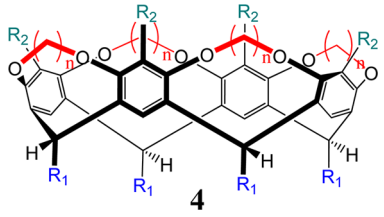

In this work, we aimed at investigating quantitatively the validity of the theoretical gas-oriented model, described in ref 6, in the prediction of the NLO properties of multichromophoric cavitands based on resorcin[4]arenes (Chart 2). For this reason, we designed and synthesized a series of new cavitands functionalized with four push–pull subchromophores that are aligned in a parallel fashion. The novel molecules are fully characterized, and their NLO properties are evaluated by electric field-induced second harmonic generation (EFISHG) measurements. To the best of our knowledge, this work shows for the first time the design of NLO-active cavitands based on the optimization of both the intramolecular chromophore order and the interdipolar opening angle.

2. EXPERIMENTAL AND THEORETICAL METHODS

General Methods. In this study, tetra(ethynyl)cavitand (**5**)[28] was used as substrate in fourfold Sonogashira reactions to access multichromophoric NLO cavitands (**6–9**). The full characterization of **6** was reported in ref 26. Chemicals, including 4-ethynyl-1-benzyloxybenzene, were purchased from Sigma-Aldrich and used without further purifications. ^{1}H and ^{13}C NMR spectra were recorded at 25 °C in $CDCl_3$ (or in DMSO-d_6) on a Bruker 500 MHz spectrometer. The ^{1}H chemical shifts (δ), reported in parts per million (ppm) downfield, are referenced to the residual protons (7.26 ppm for $CDCl_3$ and 2.50 for DMSO-d_6). The ^{13}C chemical shifts are referenced to the carbon resonance of $CDCl_3$ (77.00 ppm) or to that of DMSO-d_6 (39.52 ppm), respectively. Mass spectra of

DOI: 10.1021/acs.jpcc.5b03047
J. Phys. Chem. C 2015, 119, 12608–12615

the new cavitands were obtained on a Waters Micromass LCT Premier Mass Spectrometer in positive ion mode (TOF-MS-ES$^+$). High-resolution mass spectra of the reference compounds were obtained on an Agilent 6530 Series Q-TOF LC/MS system in negative ion mode (ESI-QTOF). The quadratic hyperpolarizabilities were measured using the electric-field-induced second harmonic generation (EFISHG) technique, which is fully described in the Supporting Information.

*General Procedure for the Synthesis of Cavitands **6**–**9**.* Tetra(ethynyl)cavitand **5** (111 mg, 0.1 mmol), $Pd(OAc)_2$ (5.6 mg, 0.025 mmol), PPh_3 (13.1 mg, 0.05 mmol), and CuI (20 mg, 0.1 mmol) were placed under an inert atmosphere into a Schlenk tube, and deoxygenated THF (30 mL) was added. Then, 0.4 mmol of the corresponding coupling partner was added to the reaction mixture: iodobenzene (45 μL) for cavitand **6**, 4-iodobenzotrifluoride (59 μL) for cavitand **7**, 4-iodobenzonitrile (92 mg) for cavitand **8**, and 1-iodo-4-nitrobenzene (100 mg) for cavitand **9**, respectively. K_2CO_3 (116 mg, 0.84 mmol) was dissolved in deoxygenated water (5 mL) and added to the reaction mixture, which was then stirred at 65 °C for 16 h. In the case of tetrakis(4-nitrophenylethynyl)-cavitand (**9**), the pure product was precipitated, collected by filtration, and dried in vacuo. Otherwise, the reaction mixture was partitioned between CH_2Cl_2 (40 mL) and water (40 mL). The organic phase was separated, and the aqueous phase was extracted with another portion of CH_2Cl_2 (20 mL). The combined organic phases were washed with water (30 mL), dried over $MgSO_4$, and evaporated to dryness. Reprecipitation from CH_2Cl_2/MeOH afforded the pure products (**6**–**8**).

*General Procedure for the Synthesis of Model Compounds **10**–**13**.* 4-Ethynyl-1-benzyloxybenzene (100 mg, 0.48 mmol), $Pd(OAc)_2$ (5.6 mg, 0.025 mmol), PPh_3 (13.1 mg, 0.05 mmol), and CuI (30 mg, 0.15 mmol) were dissolved in deoxygenated THF (30 mL) under an inert atmosphere into a Schlenk tube. Then, 0.48 mmol of the corresponding coupling partner was added to the reaction mixture: iodobenzene (55 μL) for compound **10**, 4-iodobenzotrifluoride (71 μL) for compound **11**, 4-iodobenzonitrile (110 mg) for compound **12**, and 1-iodo-4-nitrobenzene (120 mg) for compound **13**, respectively. K_2CO_3 (133 mg, 0.96 mmol) was dissolved in deoxygenated water (5 mL). This solution was also added to the reaction mixture, which was then stirred at 65 °C for 48 h. The reaction mixture was partitioned between CH_2Cl_2 (40 mL) and water (40 mL). The organic phase was separated, and the aqueous phase was extracted with another portion of CH_2Cl_2 (20 mL). The combined organic phases were washed with water (30 mL), and the solvent was removed on a rotary evaporator. The crude products were purified by column chromatography on silica gel.

*Tetrakis(4-trifluoromethylphenylethynyl)cavitand (**7**).* Brown solid (97 mg, 57%); mp 310 °C (dec.). Found: C, 71.36; H, 4.28. $C_{100}H_{68}F_{12}O_{12}$ requires C, 71.09; H, 4.06; ν_{max}(KBr): 973, 1066, 1125, 1247, 1323, 1503, 1602, 2216 cm^{-1}; λ_{max}(UV–vis): 298 nm; δ_H (500.15 MHz, $CDCl_3$): 1.84 (12H, d, J 7.0 Hz, CH_3CH), 4.67 (4H, d, J 6.9 Hz, inner of OCH_2O), 4.97 (8H, s, ArCH_2O), 5.11 (4H, q, J 7.0 Hz, CH$_3$CH), 5.80 (4H, d, J 6.9 Hz, outer of OCH_2O), 6.90 (8H, d, 8.2 Hz, Ar), 7.42 (4H, s, Ar), 7.48 (8H, d, 8.2 Hz, Ar), 7.51–7.60 (16H, m, Ar); δ_C (125.78 MHz, $CDCl_3$): 16.2 (*C*H$_3$CH), 31.20 (CH$_3$*C*H), 60.7 (Ar*C*H$_2$O), 87.1 (Ar–*C*≡C), 91.6 (C≡*C*–C$_6$H$_4$CF$_3$), 100.1 (O*C*H$_2$O), 114.6, 115.2, 120.8, 122.3, 123.9 (q, $^1J_{(C-F)}$ 272 Hz), 125.2, 127.3, 129.7 (q, $^2J_{(C-F)}$ 32 Hz), 131.6, 133.4, 139.0, 154.0, 159.0. TOF-MS-ES$^+$: 1712.4 [M+23]$^+$.

*Tetrakis(4-cyanophenylethynyl)cavitand (**8**).* Yellow solid (121 mg, 80%); mp 280 °C (dec.). Found: C, 79.38; H, 4.68. $C_{100}H_{68}N_4O_{12}$ requires C, 79.14; H, 4.52; ν_{max}(KBr): 975, 1247, 1513, 1598, 2215, 2226 cm^{-1}; λ_{max}(UV–vis): 315 nm; δ_H (500.15 MHz, $CDCl_3$): 1.84 (12H, d, J 7.3 Hz, CH_3CH), 4.65 (4H, d, J 7.2 Hz, inner of OCH_2O), 4.96 (8H, s, ArCH_2O), 5.11 (4H, q, J 7.3 Hz, CH$_3$CH), 5.78 (4H, d, J 7.2 Hz, outer of OCH_2O), 6.90 (8H, d, 8.7 Hz, Ar), 7.42 (4H, s, Ar), 7.48 (8H, d, 8.7 Hz, Ar), 7.52–7.61 (16H, m, Ar); δ_C (125.78 MHz, $CDCl_3$): 16.2 (*C*H$_3$CH), 31.3 (CH$_3$*C*H), 60.7 (Ar*C*H$_2$O), 87.0 (Ar–*C*≡C), 93.7 (C≡*C*–C$_6$H$_4$NO$_2$), 100.0 (O*C*H$_2$O), 111.3, 114.7, 114.8, 118.4, 120.9, 122.2, 128.4, 131.8, 132.0, 133.5, 139.0, 154.0, 159.3. TOF-MS-ES$^+$: 1540.4 [M+23]$^+$.

*Tetrakis(4-nitrophenylethynyl)cavitand (**9**).* Light brown solid (92 mg, 58%); mp 300 °C (dec.). Found: C, 72.33; H, 4.41, N, 3.65. $C_{96}H_{68}N_4O_{20}$ requires C, 72.17; H, 4.29; N, 3.51. ν_{max}(KBr): 975, 1247, 1342, 1511, 1591, 2214 cm^{-1}; δ_H (500.15 MHz, DMSO-d_6): 1.90 (12H, br s, CH_3CH), 4.48 (4H, br s, inner of OCH_2O), 4.90 (12H, br s, ArCH_2O overlapping with CH$_3$CH), 5.81 (4H, br s, outer of OCH_2O), 6.99 (8H, br s, Ar), 7.54 (8H, br s, Ar), 7.71 (8H, br s, Ar) 7.92 (4H, br s, Ar), 8.16 (8H, br s, Ar). TOF-MS-ES$^+$: 1619.4 [M+23]$^+$.

*1-Phenylethynyl-4-benzyloxybenzene (**10**).* Light yellow solid (40 mg, 29%); R_f: 0.5 (toluene/*n*-hexane = 1/1); mp 105–107 °C; ν_{max}(KBr): 2216 cm^{-1}; λ_{max}(UV–vis): 291 nm; δ_H (500.15 MHz, $CDCl_3$): 5.12 (2H, s, CH_2); 6.99 (2H, d, 8.7 Hz, C$_6H_4$); 7.35 (2 H, d, 7.59 Hz, C$_6H_4$); 7.36–7.55 (10 H, m, Ph); δ_C (125.78 MHz, $CDCl_3$): 70.1; 88.2; 89.3; 115.0; 115.9; 123.6; 127.5; 127.9; 128.1; 128.3; 128.6; 131.5; 133.1; 136.6; 158.8. HR-MS: M$^+$(found): 284.1168 (C$_{21}$H$_{16}$O requires 284.1201).

*1-(4-Trifluoromethylphenylethynyl)-4-benzyloxybenzene (**11**).* Brown solid (40 mg, 23%); R_f: 0.6 (CH$_3$Cl/toluene =1/1); mp 132–134 °C; ν_{max}(KBr): 2222 cm^{-1}; λ_{max}(UV–vis): 300 nm; δ_H (500.15 MHz, $CDCl_3$): 5.12 (2H, s, CH_2); 7.00 (2H, d, 8.7 Hz, C$_6H_4$); 7.33–7.48 (5H, m, Ph); 7.50 (2H, d, 8.7 Hz, C$_6H_4$); 7.62 (4H, br s, C$_6H_4$); δ_C (125.78 MHz, $CDCl_3$): 70.1; 86.9; 91.9; 114.9; 115.0; 124.1 (q, $^1J_{(C-F)}$ 287 Hz); 125.3; 127.5; 128.1; 128.7; 129.6; 129.8; 131.6; 133.3; 136.5; 159.2. HR-MS: M$^+$(found): 352.1035 (C$_{22}$H$_{15}$OF$_3$ requires 352.1075).

*1-(4-Cyanophenylethynyl)-4-benzyloxybenzene (**12**).* Yellow solid (50 mg, 33%); R_f: 0.6 (CH$_3$Cl/toluene =1/1); mp 135–137 °C; ν_{max}(KBr) 2228, 2220 cm^{-1}; λ_{max}(UV–vis): 319 nm; δ_H (500.15 MHz, $CDCl_3$): 5.12 (2H, s, CH_2); 7.00 (2H, d, 8.4 Hz, C$_6H_4$); 7.35–7.50 (5H, m, Ph); 7.50 (2H, d, 8.4 Hz, C$_6H_4$); 7.61 (4H, dd, 22.8 Hz, 7.8 Hz, C$_6H_4$); δ_C (125.78 MHz, $CDCl_3$): 70.1; 86.8; 94.1; 111.1; 111.8; 114.8; 115.1; 118.5; 127.5; 128.2; 128.7; 132.0; 132.1; 133.4; 136.4; 159.5. HR-MS: M$^+$(found): 309.1111 (C$_{22}$H$_{15}$NO requires 309.1154).

*1-(4-Nitrophenylethynyl)-4-benzyloxybenzene (**13**).* Orange solid (50 mg, 31%); R_f: 0.6 (CH$_3$Cl/toluene =1/1); mp 137–139 °C; ν_{max}(KBr) 2220 cm^{-1}; δ_H (500.15 MHz, $CDCl_3$): 5.13 (2H, s, CH_2); 7.02 (2H, d, 7.6 Hz, C$_6H_4$); 7.45–7.53 (3H, m, C$_6H_4$); 7.53 (2H, d, 7.6 Hz, C$_6H_4$); 7.7 (2H, d, 7.8 Hz, C$_6H_4$); 7.95 (2H, m, C$_6H_4$); 8.24 (2H, d, 7.6 Hz, C$_6H_4$); δ_C (125.78 MHz, $CDCl_3$): 70.1; 86.7; 95.1; 111.8; 114.5; 115.1; 126.7; 124.7; 127.5; 128.7; 130.7; 132.0; 133.5; 136.4; 159.6. HR-MS: M$^+$(found): 329.1009 (C$_{21}$H$_{15}$NO$_3$ requires 329.1052).

DOI: 10.1021/acs.jpcc.5b03047
J. Phys. Chem. C 2015, 119, 12608–12615

Scheme 1. Synthesis of (a) the Multichromophoric Cavitands 6−9 and (b) the Monochromophoric Reference Compounds 10−13 via Sonogashira Coupling Reactions

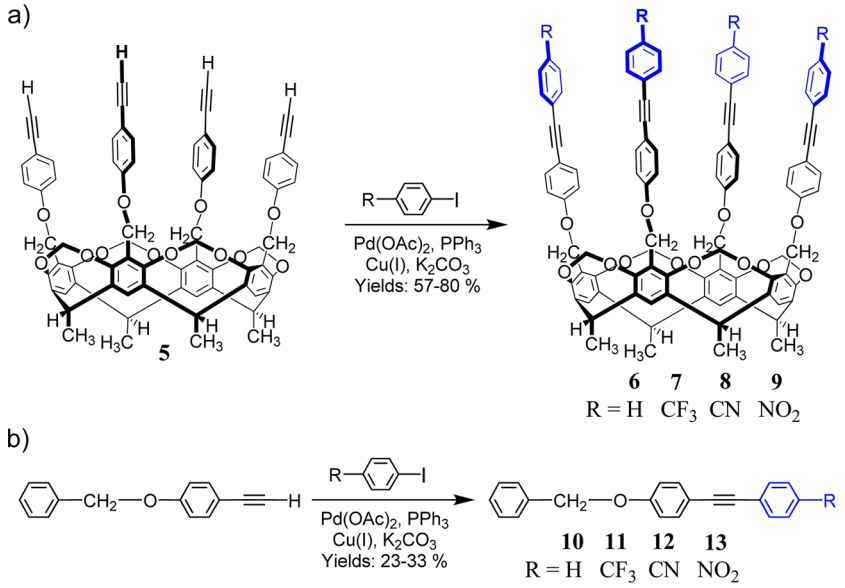

Computational Methods. Optimized geometries of **6**−**13** were obtained by carrying out a conformational search using the Schrödinger Suite[29] with the force field MM3, followed by the use of the semiempirical PM6 Hamiltonian method.[30] The solvent (chloroform) effect was also considered in the semiempirical calculation by the application of the COSMO model.[31] Further details about the theoretical procedure, together with all optimized structures, are shown in the Supporting Information.

3. RESULTS AND DISCUSSION

Cavitand **5** was reacted with iodobenzene or para-substituted iodobenzenes (4-iodobenzotrifluoride, 4-iodobenzonitrile, 1-iodo-4-nitrobenzene) in the presence of copper(I)iodide, potassium carbonate, and $Pd(OAc)_2$ + 2 PPh_3 in situ catalytic system (Scheme 1). All reactions afforded cleanly the expected products (**6**−**9**) in good yields (57−80%). The synthetic strategy used here has enabled one to achieve a rapid diversification of this cavitand family by implementing electron-withdrawing groups (CF_3, CN, and NO_2) at the upper edge of the conjugated π-system (Scheme 1). In contrast to the calixarene-based compounds (**1**−**3**), the macrocyclic ring itself is not part of the extended multichromophoric system, but it simply provides a rigid molecular scaffold to which the four dipolar NLO subunits are directly attached. Using analogous synthetic protocols, the corresponding monochromophoric reference compounds (**10**−**13**) were also synthesized from the commercially available 4-ethynyl-1-benzyloxybenzene (Scheme 1). These model compounds have structural motives identical to those of the individual chromophoric subunits in each corresponding cavitand product.

In their UV−vis spectra, the novel cavitands **7** and **8** show a small blue shift of 2 and 4 nm, respectively, when compared to their monomeric reference compounds **11** and **12** (Table 1 and Table 2), thus maintaining the transparency window in the visible spectral region and the possible applicability of these materials. This hypsochromic shift is indicative of weak intramolecular interactions or aggregation effects between the subchromophores within these multichromophoric systems.[20,32] The quadratic hyperpolarizabilities ($\mu\beta$) of both the macrocyclic chromophores and the reference model compounds were evaluated by EFISHG with a fundamental wavelength of 1910 nm.[33] The second harmonic response of the tetrakis(4-nitrophenylethynyl)cavitand (**9**), which accommodates groups with the strongest electron-withdrawing effect,

Table 1. Maximum Absorption Wavelengths, Average Opening Angles Obtained from MM, and Experimental and Theoretical (Gas-Oriented Model) Static Quadratic Hyperpolarizabilities for Cavitands 6−8

	experimental		MM[b]	gas-oriented model
compound (R)	λ_{max} (nm)	$\mu\beta_0$[a] (10^{-48} esu)	θ_{avg} (deg)	$\mu\beta_0$ (10^{-48} esu)
6 (H)	291	320	1	368
7 (CF_3)	298	320	5	479
8 (CN)	315	360	17	799

[a]EFISHG with a fundamental wavelength of 1910 nm; all measurements were performed in $CHCl_3$ at room temperature; the relative experimental error for the $\mu\beta_0$ values is 10%. [b]PM6 method with chloroform solvent (COSMO).

Table 2. Maximum Absorption Wavelengths, Dipole Moments, and Experimental and Theoretical (Molecular Modeling) Static Quadratic Hyperpolarizabilities for Monochromophoric Reference Compounds 10−12

	experimental		MM[b]		
compound (R)	λ_{max} (nm)	$\mu\beta_0$[a] (10^{-48} esu)	μ (D)	β_0 (10^{-30} esu)	$\mu\beta_0$ (10^{-48} esu)
10 (H)	291	23	2.2	8.4	19
11 (CF_3)	300	30	1.6	18.0	29
12 (CN)	319	60	3.8	17.4	66

[a]EFISHG with a fundamental wavelength of 1910 nm; all measurements were performed in $CHCl_3$ at room temperature; the relative experimental error for the $\mu\beta_0$ values is 10%. [b]PM6 method with chloroform solvent (COSMO).

DOI: 10.1021/acs.jpcc.5b03047
J. Phys. Chem. C 2015, 119, 12608−12615

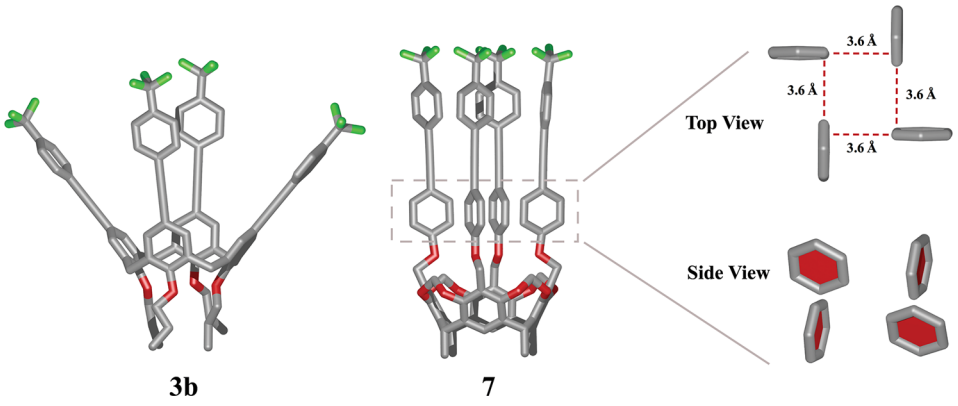

Figure 1. Energy-minimized structures of calixarene **3b** and cavitand **7**. Hydrogens are omitted for clarity. The red dashed lines represent T-shaped edge-to-face interactions between the neighboring aromatic rings.

could not be determined due to its limited solubility in organic solvents.

The measured quadratic hyperpolarizabilities were corrected by a dispersion factor derived from a two-level model, which allows the determination of static quadratic hyperpolarizabilities.[34,35] The resonance-corrected $\mu\beta_0$ values for the cavitands **6**–**8** and for the model compounds **10**–**12** are given in Table 1 and 2, respectively. Cavitand **6**, lacking acceptor groups at the end of its conjugated π-system, shows a $\mu\beta_0$ value of 320 × 10^{-48} esu. The incorporation of neither trifluoromethyl nor nitrile groups increased significantly the quadratic hyperpolarizabilities: $\mu\beta_0$ values of 320 × 10^{-48} esu and 360 × 10^{-48} esu were obtained for cavitands **7** and **8**, respectively. In contrast, the $\mu\beta_0$ values of the corresponding reference compounds **10**–**12** increase with the inclusion of electron-withdrawing groups. An enhancement factor of 3.5 per chromophore was calculated for compound **6**, which is among the highest values observed for multichromophoric NLO macrocycles (the maximum theoretical enhancement is 4).

Semiempirical PM6 molecular modeling (MM) was carried out for the new compounds as described in the Supporting Information. The calculations revealed that the average opening angle (θ_{avg}) is very small for compounds **6** (1°) and **7** (5°), which indicates a nearly parallel alignment of the four subchromophoric building blocks in these new derivatives. On the other hand, the aperture angle is somewhat higher (17°) for cavitand **8** as shown in Table 1. The dihedral angles between the planes involving the neighboring rings are approximately 90° for both the middle and the upper row of phenyls in all cavitand derivatives. The average shortest distances between the aromatic carbon atoms of the neighboring subchromophores of the same cavitand were found to be 3.6, 3.6, and 4.4 Å for the middle row of aromatic rings of cavitands **6**, **7**, and **8**, respectively. The same distances for the upper row of phenyl rings were 3.6, 3.7, and 6.8 Å for **6**, **7** and **8**, respectively. The side view and top view of the middle-row aromatic rings obtained from the PM6-optimized structure of **7** are shown in Figure 1. Therefore, the observed short noncontact distances, which are combined with the nearly perpendicular arrangements of the neighboring aromatic rings (Figure 1), suggest that edge-to-face T-shaped interactions are the major forces that stabilize these new multichromophoric NLO cavitands in their conformations.[36−38] The self-organization of the aromatic building blocks on the different levels of the extended π-system results in a highly ordered arrangement for these molecules. Similarly, both X-ray crystallographic studies and gas-phase theoretical calculations revealed the presence of weak perpendicular T-shaped interactions between the upper phenyl rings of a related deepened cavitand.[25] Furthermore, an upfield shift of 0.1 ppm was observed in ^{1}H NMR for the separated aromatic proton resonances of the middle row of phenyl rings in cavitands **6**–**8** (6.90 ppm) when compared to the same proton signals in model compounds **10**–**12** (7.00 ppm), which is a clear indication of the presence of such intramolecular interactions.[39,40]

For comparison, we also computed the energy-minimized structures for the calix[4]arenes analogues **3a**–**c** (see Supporting Information). In accordance with the reported X-ray structures, all these derivatives adopt a typical pinched cone conformer, where two opposite subunits in the 1,3-positions are almost parallel, while those in the 2,4-positions bend out with an approximate angle of 45°. The authors claimed that neither in the single molecule nor in the crystal packing were the typical distances indicative for attractive interactions such as π–π stacking observed.[12,13] The energy-minimized structures of the trifluoromethyl derivatives **3b** and **7** are given in Figure 1, which shows marked differences between their structural geometries. For instance, the average opening angles were found to be 24° and 5° for calixarene **3b** and cavitand **7**, respectively. Therefore, the contribution of intramolecular interactions to the control of the NLO response may be more effective in the newly developed cavitands **6**–**9** than in classical calixarenes due to the more parallel orientations of the four monochromophoric subunits.

The inclusion of the solvent effect (COSMO model) in the semiempirical PM6 calculations enabled us to perform high-precision computations to determine the theoretical dipole moments and the quadratic hyperpolarizabilities for the monochromophoric model compounds **10**–**12** (Table 2). Since the experimentally determined $\mu\beta_{mono}$ values of the reference compounds were in excellent agreement with the calculated ones, we can safely apply these values in eq 3, together with the opening angles derived from the molecular modeling, in order to determine the quadratic hyperpolarizabilities of our multichromophoric cavitands based on the gas-oriented model.[16] According to this simple approximation, which neglects nonbonding electronic interactions between the individual NLO subunits, $\mu\beta_{multi}$ = 368, 479, and 799 × 10^{-48} esu were calculated for compounds **6**, **7**, and **8**, respectively (Table 1). The comparison of these values to the experimental ones revealed a significant decrease in the quadratic hyper-

DOI: 10.1021/acs.jpcc.5b03047
J. Phys. Chem. C 2015, 119, 12608−12615

polarizabilities for **7** (33%) and **8** (55%). On the contrary, cavitand **6** showed minor suppression (13%) in its $\mu\beta_0$ value.

Therefore, in full accordance with the prediction of the theoretical model in ref 16, a decrease in the cone angle of the cavitand with respect to that of classical calixarenes is accompanied by an increase in the suppression of the quadratic hyperpolarizabilities. We show experimentally that this effect is particularly intensified when the monochromophoric subunits possess highly dipolar character. The large deviation of the $\mu\beta_0$ values from the simple additive oriented-gas model in compounds **7** and **8** may be attributed to intramolecular cooperative and/or collective effects. Due to repulsive interactions, the strongly polarizable monochromophoric subunits reduce their polarization in response to the electric field generated by other neighboring subchromophores in their close proximity.[16−19,41,42] In addition to this cooperative behavior, collective excitonic effects resulting from the interchromophoric delocalization of the excitation have also important consequences on the material properties. In the constrained geometry of cavitands, the delocalization of the exciton states gives rise to an increase of the optical gap, which is therefore responsible for the collective suppression of the NLO responses.[16−19,41,42] It has been recently realized that cooperativity plays an important role in the organization of complex chemical systems[43,44] including supramolecular polymerization,[45,46] molecular recognition.[47] and self-assembly[48] as well as in organic electro-optic materials.[49,50] We believe that our finding will contribute to the better understanding of the phenomenon of cooperativity in new molecular materials with promising NLO properties.

4. CONCLUSIONS

Highly conjugated, multichromophoric cavitand derivatives were synthesized via Sonogashira coupling, whose constrained geometries were designed to decrease both the interchromophoric flexibility and the interdipolar opening angle. Theoretical calculations based on the semiempirical PM6 model indicate the presence of edge-to-face T-shaped interactions between the aromatic building blocks within these multichromophoric systems, which is further supported by the detection of hypsochromic shifts in UV−vis and upfield aromatic chemical shifts in ^{1}H NMR. The quadratic hyperpolarizability values were experimentally determined by EFISHG for the novel donor−acceptor functionalized cavitands and for their corresponding monochromophoric reference compounds. We have proved for the first time that the gain in the quadratic hyperpolarizabilities of multichromophoric NLO macrocycles, originating from the near parallel orientations of the subchromophores, can be partially canceled by electrostatic damping effects. This nonadditive behavior may arise from intramolecular cooperative and/or collective effects between the highly polar NLO tails. It is evident from this study that the elaborate interplay of many different factors renders the rational design of new supramolecular NLO materials particularly difficult. Future designs will not only require the proper choice of dipolar building blocks and the smart optimization of structural geometries, e.g., the interdipolar opening angle, but it will also be essential to take into account the effect of through-space electrostatic and/or dispersion interactions between the monochromophoric subunits.

■ ASSOCIATED CONTENT

Supporting Information

Details of the nonlinear optical measurements; description of the theoretical calculations along with all optimized structures as well as the ^{1}H and the ^{13}C NMR spectra of the new compounds. The Supporting Information is available free of charge on the ACS Publications website at DOI: 10.1021/acs.jpcc.5b03047.

■ AUTHOR INFORMATION

Corresponding Author

*E-mail: zscsok@iqsc.usp.br. Tel.: +55 16 3373-6652. Fax: +55 16 3373-9903.

Notes

The authors declare no competing financial interest.

¶E-mail: isabelle.ledoux@lpqm.ens-cachan.fr

■ ACKNOWLEDGMENTS

Dedicated to the memory of Prof. Adolfo Zambelli (Università degli Studi di Salerno). Financial support from Brazilian Agencies CNPq (400112/2014-0: *Functional Molecular Containers*), CAPES (A061_2013), and FAPESP (2014/02071-5) are gratefully acknowledged. The authors appreciate the support of the *New Széchenyi Plan* (SROP-4.2.2.A-11/1/KONV-2012-0065: *Synthesis of supramolecular systems, examination of their physicochemical properties and their utilization for separation and sensor chemistry*) and the *Hungarian National Research Fund* (OTKA, K113177). Finally, the authors thank Michael Reynolds (LPQM-ENS) for his contribution to the EFISHG measurements, as well as Tímea R. Kégl (University of Pécs) and Ibolya Prauda (University of Pécs) for the synthesis and for the HR-MS measurements of the reference compounds.

■ REFERENCES

(1) Chemla, D. S.; Zyss, J. *Nonlinear Optical Properties of Organic Molecules and Crystals*; Academic Press: New York, 1987.

(2) Nalwa, H. S.; Miyata, S. *Nonlinear Optics of Organic Molecules and Polymers*; CRC Press: New York, 1997.

(3) Prasad, P. N.; Williams, D. J. *Introduction to Nonlinear Optical Effects in Organic Molecules and Polymers*; Wiley: New York, 1991.

(4) Delgado, M. C. R.; Casado, J.; Hernández, V.; Navarrete, J. T. L.; Orduna, J.; Villacampa, B.; Alicante, R.; Raimundo, J.-M.; Blanchard, P.; Roncali, J. Electronic, Optical, and Vibrational Properties of Bridged Dithienylethylene-Based NLO Chromophores. *J. Phys. Chem. C* **2008**, *112*, 3109−3120.

(5) Ronchi, M.; Pizzotti, M.; Biroli, A. O.; Righetto, S.; Ugo, R.; Mussini, P.; Cavazzini, M.; Lucenti, E.; Salsa, M.; Fantucci, P. Second-Order Nonlinear Optical (NLO) Properties of a Multichromophoric System Based on an Ensemble of Four Organic NLO Chromophores Nanoorganized on a Cyclotetrasiloxane Architecture. *J. Phys. Chem. C* **2009**, *113*, 2745−2760.

(6) Rekaï, E. D.; Baudin, J.-B.; Jullien, L.; Ledoux, I.; Zyss, J.; Blanchard-Desce, M. A. Hyperpolar, Multichromophoric Cyclodextrin Derivative: Synthesis and Linear and Nonlinear Optical Properties. *Chem.—Eur. J.* **2001**, *7*, 4395−4402.

(7) Put, E. J. H.; Clays, K.; Persoons, A.; Biemans, H. A. M.; Luijkx, C. P. M.; Meijer, E. W. The Symmetry of Functionalized Poly(propylene imine) Dendrimers Probed with Hyper-Rayleigh Scattering. *Chem. Phys. Lett.* **1996**, *260*, 136−141.

(8) Kelderman, E.; Derhaeg, L.; Heesink, G. J. T.; Verboom, W.; Engbersen, J. F. J.; van Hulst, N. F.; Persoons, A.; Reinhoudt, D. N. Nitrocalix[4]arenes as Molecules for Second-Order Nonlinear Optics. *Angew. Chem., Int. Ed.* **1992**, *31*, 1075−1077.

(9) Kelderman, E.; Derhaeg, L.; Verboom, W.; Engbersen, J. F. J.; Harkema, S.; Persoons, A.; Reinhoudt, D. N. Calix[4]arenes as Molecules for Second Order Nonlinear Optics. *Supramol. Chem.* **1993**, *2*, 183−190.
(10) Kenis, P. J. A.; Noordman, O. F. J.; Houbrechts, S.; van Hummel, G. J.; Harkema, S.; van Veggel, F. C. J. M.; Clays, K.; Engbersen, J. F. J.; Persoons, A.; van Hulst.; et al. Second-Order Nonlinear Optical Properties of the Four Tetranitrotetrapropoxycalix[4]arene Conformers. *J. Am. Chem. Soc.* **1998**, *120*, 7875−7883.
(11) Kenis, P. J. A.; Kerver, E. G.; Snellink-Ruell, B. H. M.; van Hummel, G. J.; Harkema, S.; Flipse, M. C.; Woudenberg, R. H.; Engbersen, J. F. J.; Reinhoudt, D. N. High Hyperpolarizabilities of Donor−π−Acceptor-Functionalized Calix[4]arene Derivatives by Preorganization of Chromophores. *Eur. J. Org. Chem.* **1998**, 1089−1098.
(12) Hennrich, G.; Murillo, M. T.; Prados, P.; Song, K.; Asselberghs, I.; Clays, K.; Persoons, A.; Benet-Buchholz, J.; de Mendoza, J. Tetraalkynyl Calix[4]arenes with Advanced NLO Properties. *Chem. Commun.* **2005**, 2747−2749.
(13) Hennrich, G.; Murillo, M. T.; Prados, P.; Al-Saraierh, H.; El-Dali, A.; Thompson, D. W.; Collins, J.; Georghiou, P. E.; Teshome, A.; Asselberghs, I.; et al. Alkynyl Expanded Donor−Acceptor Calixarenes: Geometry and Second-Order Nonlinear Optical Properties. *Chem.—Eur. J.* **2007**, *13*, 7753−7761.
(14) Gutsche, C. D. *Calixarenes Revisited: Monographs in Supramolecular Chemistry*; Royal Society of Chemistry: London, 1998.
(15) Böhmer, V. Calixarenes, Macrocycles with (Almost) Unlimited Possibilities. *Angew. Chem., Int. Ed. Engl.* **1995**, *34*, 713−745.
(16) Datta, A.; Terenziani, F.; Painelli, A. Cooperative Interactions in Supramolecular Aggregates: Linear and Nonlinear Responses in Calix[4]arenes. *ChemPhysChem.* **2006**, *7*, 2168−2174.
(17) Painelli, A.; Terenziani, F. Multielectron Transfer in Clusters of Polar-Polarizable Chromophores. *J. Am. Chem. Soc.* **2003**, *125*, 5624−5625.
(18) Terenziani, F.; Painelli, A. Supramolecular Interactions in Clusters of Polar and Polarizable Molecules. *Phys. Rev. B* **2003**, *68*, 165405.
(19) Terenziani, F.; Painelli, A. Collective and Cooperative Phenomena in Molecular Materials: Dimers of Polar Chromophores. *J. Lumin.* **2005**, *112*, 474−478.
(20) Bruyère, E.; Persoons, A.; Brédas, J. L. Geometric Structure and Second-Order Nonlinear Optical Response of Substituted Calix[4]-arene Molecules: A Theoretical Study. *J. Phys. Chem. A* **1997**, *101*, 4142−4148.
(21) Di Bella, S.; Ratner, M. A.; Marks, T. J. Design of Chromophoric Molecular Assemblies with Large Second-Order Optical Nonlinearities. A Theoretical Analysis of the Role of Intermolecular Interactions. *J. Am. Chem. Soc.* **1992**, *114*, 5842−5849.
(22) Timmerman, P.; Verboom, W.; Reinhoudt, D. N. Resorcinarenes. *Tetrahedron* **1996**, *52*, 2663−2704.
(23) Botta, B.; Cassani, M.; D'Acquarica, I.; Subissati, D.; Zappia, G.; Delle Monache, G. Resorcarenes: Hollow Building Blocks for the Host−Guest Chemistry. *Curr. Org. Chem.* **2005**, *9*, 1167−1202.
(24) Cram, D. J.; Karbach, S.; Kim, H. E.; Knobler, C. B.; Maverick, E. F.; Ericson, J. L.; Helgeson, R. C. Host−Guest Complexation. 46. Cavitands as Open Molecular Vessels Form Solvates. *J. Am. Chem. Soc.* **1988**, *110*, 2229−2237.
(25) Csók, Z.; Kégl, T.; Párkányi, L.; Varga, Á.; Kunsági-Máté, S.; Kollár, L. Facile, High-Yielding Synthesis of Deepened Cavitands: A Synthetic and Theoretical Study. *Supramol. Chem.* **2011**, *23*, 710−719.
(26) Csók, Z.; Takátsy, A.; Kollár, L. Highly Selective Palladium-Catalyzed Aminocarbonylation and Cross-Coupling Reactions on a Cavitand Scaffold. *Tetrahedron* **2012**, *68*, 2657−2661.
(27) Li, Y.; Csók, Z.; Szuroczki, P.; Kollár, L.; Kiss, L.; Kunsági-Máté, S. Fluorescence Quenching Studies on the Interaction of a Novel Deepened Cavitand Towards Some Transition Metal Ions. *Anal. Chim. Acta* **2013**, *799*, 51−56.
(28) Csók, Z.; Kégl, T.; Li, Y.; Skoda-Földes, R.; Kiss, L.; Kunsági-Máté, S.; Todd, M. H.; Kollár, L. Synthesis of Elongated Cavitands via Click Reactions and Their Use as Chemosensors. *Tetrahedron* **2013**, *69*, 8186−8190.
(29) Schrödinger Release 2014-3: MacroModel, version 10.5, Schrödinger, LLC, New York, 2014.
(30) Stewart, J. J. P. Optimization of Parameters for Semiempirical Methods V: Modification of NDDO Approximations and Application to 70 Elements. *J. Mol. Model.* **2007**, *13*, 1173−1213.
(31) Klamt, A.; Schüürmann, G. COSMO: A New Approach to Dielectric Screening in Solvents with Explicit Expressions for the Screening Energy and its Gradient. *J. Chem. Soc., Perkin Trans.* **1993**, *2*, 799−805.
(32) Knoester, J. In *Organic Nanostructures: Science and Applications*; Agranovich, W. M., La Rocca, G. C., Eds.; IOS Press: Amsterdam, 2002; p 149.
(33) Ledoux, I.; Zyss, J. Influence of the Molecular Environment in Solution Measurements of the Second-Order Optical Susceptibility for Urea and Derivatives. *Chem. Phys.* **1982**, *73*, 203−213.
(34) Oudar, J. L. Optical Nonlinearities of Conjugated Molecules. Stilbene Derivatives and Highly Polar Aromatic Compounds. *J. Chem. Phys.* **1977**, *67*, 446−457.
(35) Oudar, J. L.; Chemla, D. S. Hyperpolarizabilities of the Nitroanilines and Their Relations to the Excited State Dipole Moment. *J. Chem. Phys.* **1977**, *66*, 2664−2668.
(36) Meyer, E. A.; Castellano, R. K.; Diederich, F. Interactions with Aromatic Rings in Chemical and Biological Recognition. *Angew. Chem., Int. Ed.* **2003**, *42*, 1210−1250.
(37) Salonen, L. M.; Ellermann, M.; Diederich, F. Aromatic Rings in Chemical and Biological Recognition: Energetics and Structures. *Angew. Chem., Int. Ed.* **2011**, *50*, 4808−4842.
(38) Martinez, C. R.; Iverson, B. L. Rethinking the Term "Pi-Stacking". *Chem. Sci.* **2012**, *3*, 2191−2201 and references therein..
(39) Mitchell, R. H. Measuring Aromaticity by NMR. *Chem. Rev.* **2001**, *101*, 1301−1315.
(40) Chou, T.-C.; Huang, J.-K.; Bahekar, S. S.; Liao, J.-H. Quinoxaline-Walled π-Stacking Molecules: Synthesis, Conformation, and Luminescence Properties. *Tetrahedron* **2014**, *70*, 8361−8373 and references therein..
(41) Painelli, A.; Terenziani, F. In *Nonlinear Optical Properties of Matter: From Molecules to Condensed Phases*; Papadopoulos, M. G., Sadlej, A. J., Leszczynski, J., Eds.; Springer: Heidelberg, Germany, 2006.
(42) Datta, A.; Pati, S. K. Dipolar Interactions and Hydrogen Bonding in Supramolecular Aggregates: Understanding Cooperative Phenomena for 1st Hyperpolarizability. *Chem. Soc. Rev.* **2006**, *35*, 1305−1323.
(43) Ercolani, G.; Schiaffino, L. Allosteric, Chelate, and Interannular Cooperativity: A Mise au Point. *Angew. Chem., Int. Ed.* **2011**, *50*, 1762−1768.
(44) Hunter, C. A.; Anderson, H. L. What is Cooperativity? *Angew. Chem., Int. Ed.* **2009**, *48*, 7488−7499.
(45) Aparicio, F.; García, F.; Sánchez, L. Supramolecular Polymerization of C_3-Symmetric Organogelators: Cooperativity, Solvent, and Gelation Relationship. *Chem. Eur. J.* **2013**, *19*, 3239−3248.
(46) Mayoral, M. J.; Rest, C.; Stepanenko, V.; Schellheimer, J.; Albuquerque, R. Q.; Fernández, G. Cooperative Supramolecular Polymerization Driven by Metallophilic Pd···Pd Interactions. *J. Am. Chem. Soc.* **2013**, *135*, 2148−2151.
(47) Bähring, S.; Olsen, G.; Stein, P. C.; Kongsted, J.; Nielsen, K. A. Coordination-Driven Switching of a Preorganized and Cooperative Calix[4]pyrrole Receptor. *Chem.—Eur. J.* **2013**, *19*, 2768−2775.
(48) Schaeffer, G.; Fuhr, O.; Fenske, D.; Lehn, J.-M. Self-Assembly of a Highly Organized, Hexameric Supramolecular Architecture: Formation, Structure and Properties. *Chem.—Eur. J.* **2014**, *20*, 179−186.
(49) Knorr, D. B., Jr.; Benight, S. J.; Krajina, B.; Zhang, C.; Dalton, L. R.; Overney, R. M. Nanoscale Phase Analysis of Molecular Cooperativity and Thermal Transitions in Dendritic Nonlinear Optical Glasses. *J. Phys. Chem. B* **2012**, *16*, 13793−13805.

DOI: 10.1021/acs.jpcc.5b03047
J. Phys. Chem. C 2015, 119, 12608−12615

(50) Dalton, L. R.; Benight, S. J.; Johnson, L. E.; Knorr, D. B., Jr.; Kosilkin, I.; Eichinger, B. E.; Robinson, B. H.; Jen, A. K.-Y.; Overney, R. M. Systematic Nanoengineering of Soft Matter Organic Electro-optic Materials. *Chem. Mater.* **2011**, *23*, 430−445.

DOI: 10.1021/acs.jpcc.5b03047
J. Phys. Chem. C 2015, 119, 12608−12615